

Synthesis of Ag–CoFe₂O₄ dimer colloidal nanoparticles and enhancement of their magnetic response

S. K. Sharma, G. Lopes, J. M. Vargas, L. M. Socolovsky, K. R. Pirota, and M. Knobel

Citation: *Journal of Applied Physics* **109**, 07B530 (2011); doi: 10.1063/1.3556771

View online: <http://dx.doi.org/10.1063/1.3556771>

View Table of Contents: <http://scitation.aip.org/content/aip/journal/jap/109/7?ver=pdfcov>

Published by the [AIP Publishing](#)

Articles you may be interested in

[Synthesis and characterization of CoFe₂O₄ nanoparticles with high coercivity](#)

J. Appl. Phys. **117**, 17A736 (2015); 10.1063/1.4916544

[Maximizing surface-enhanced Raman scattering sensitivity of surfactant-free Ag-Fe₃O₄ nanocomposites through optimization of silver nanoparticle density and magnetic self-assembly](#)

J. Appl. Phys. **114**, 124305 (2013); 10.1063/1.4823732

[Effect of the Zn content in the magnetic properties of Co_{1-x}Zn_xFe₂O₄ mixed ferrites](#)

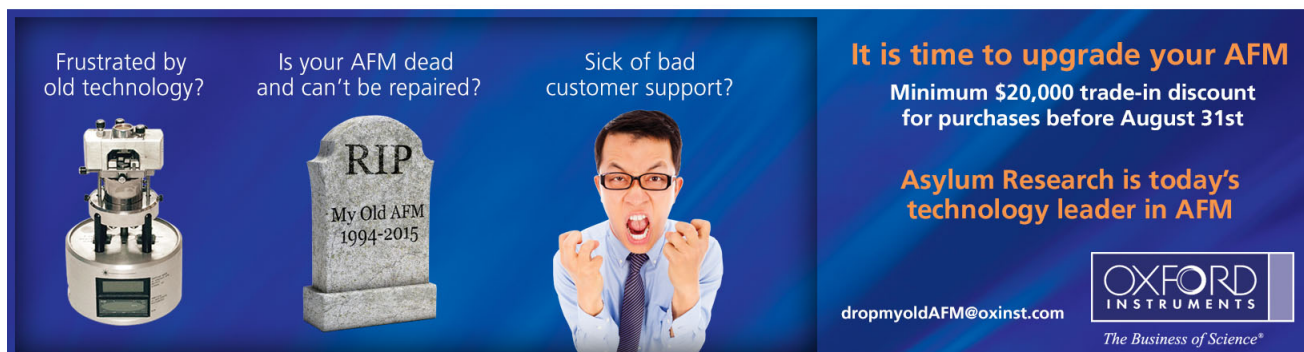
J. Appl. Phys. **113**, 17B513 (2013); 10.1063/1.4796173

[Origin of magnetic anisotropy in ZnO/CoFe₂O₄ and CoO/CoFe₂O₄ core/shell nanoparticle systems](#)

Appl. Phys. Lett. **101**, 252405 (2012); 10.1063/1.4771993

[Enhanced magnetic and dielectric properties of Eu and Co co-doped BiFeO₃ nanoparticles](#)

Appl. Phys. Lett. **101**, 042401 (2012); 10.1063/1.4738992

The advertisement is set against a dark blue background. On the left, there is a photograph of a white AFM instrument. In the center, a grey tombstone-shaped sign reads 'RIP My Old AFM 1994-2015'. To the right of the sign is a photograph of a man in a white shirt and tie, looking frustrated with his hands clenched in fists. Text on the left side asks: 'Frustrated by old technology?', 'Is your AFM dead and can't be repaired?', and 'Sick of bad customer support?'. On the right side, the text reads: 'It is time to upgrade your AFM', 'Minimum \$20,000 trade-in discount for purchases before August 31st', and 'Asylum Research is today's technology leader in AFM'. At the bottom right, the Oxford Instruments logo is displayed with the tagline 'The Business of Science®' and the email address 'dropmyoldAFM@oxinst.com'.

Synthesis of Ag–CoFe₂O₄ dimer colloidal nanoparticles and enhancement of their magnetic response

S. K. Sharma,^{1,a)} G. Lopes,¹ J. M. Vargas,² L. M. Socolovsky,³
K. R. Pirota,¹ and M. Knobel¹

¹*Instituto de Física Gleb Wataghin, Universidade Estadual de Campinas (UNICAMP), Campinas 13.083-859, Sao Paulo, Brazil*

²*Center for High Technology Materials, University of New Mexico, 1313 Goddard SE, Albuquerque, New Mexico 87106-4343, USA*

³*LSA-INTECIN, Facultad de Ingenieria, Universidad de Buenos Aires, C1063ACV, Argentina*

(Presented 17 November 2010; received 24 September 2010; accepted 24 November 2010; published online 6 April 2011)

This paper reports the structural and magnetic properties of Ag–CoFe₂O₄ colloidal dimer nanoparticles (NPs) synthesized using a two-step solution-phase route. Ag NPs were used as seeds to grow Ag–CoFe₂O₄ dimer NPs using thermal decomposition of metallic precursor. By means of temperature and field dependent dc magnetization measurements, it is found that the silver due to its interface with CoFe₂O₄ particles leads to thermal stabilization of the dimer NPs superior as compared to CoFe₂O₄ alone. Our results show enhancement of the magnetic anisotropy and a large coercivity at 2 K for dimer NPs, which could be ascribed to interface effect between Ag and CoFe₂O₄ components and the related structural defects. © 2011 American Institute of Physics. [doi:10.1063/1.3556771]

I. INTRODUCTION

The understanding of the influence of finite size effect and surface effects on magnetic properties of nanoparticles (NPs) represents an attractive area of research.¹ Additionally, the combination of electronic and magnetic responses through a dimer-type particle system allows one to study microscopically the complex and intricate interaction mechanism within the dimer structure and the possibility to tune and enhance the magnetic properties.^{2,3} Specifically, metallic NPs such as Ag and Au systems exhibit striking features that are not observed in their bulk counterparts, for example, ferromagnetism reported in Au NPs coated by protective agents, such as dodecane—thiol.⁴ Cobalt ferrite (CoFe₂O₄) is a ferrimagnetic material with a cubic inverse spinel structure represented by B(AB)O₄ where oxygen forms a fcc close packing, and the Fe cation occupies both interstitial tetrahedral (A) and octahedral sites [B] and Co cation occupy only the octahedral sites. CoFe₂O₄ NPs dispersions have been widely used as ferrofluid in, for example, rotary shaft sealing, oscillation damping, and position sensing. The use of properly coated CoFe₂O₄ NPs in clinical medicine has also intensified. Such a suspension can interact with an external magnetic field and be positioned to a specific area, facilitating magnetic resonance imaging for medical diagnosis and ac magnetic field-assisted cancer therapy.⁵

Dimer like NPs, that is, CoFe₂O₄ particles attached to metallic and non-magnetic particles, such as Ag or Au provide NPs stability in solution and help in binding various biological ligands to the NPs surface. Thus, they could be used as nanovectors for drug delivery with convenient enhancement of both optical and magnetic properties.⁶

Therefore, the proposition of a method for designing particles with the physical properties of Ag NPs composition but with the chemistry of CoFe₂O₄ would represent a major advance. Here, we describe a solution-phase route to prepare Ag–CoFe₂O₄ colloidal dimer NPs. The structural and magnetic results show the enhancement of the magnetic anisotropy and coercivity, which could be ascribed to interface effect and the related structural defects.

II. EXPERIMENTAL DETAILS

We have used a two-step chemical route for the synthesis of Ag–CoFe₂O₄ colloidal NPs as described in detail elsewhere for Ag–Fe₃O₄ dimer NPs.³ In each synthesis, the prepared mixture was gently heated to the final temperature of 260 °C for 60 min under an inert atmosphere. The solution mixture was then cooled to room temperature and colloidal NPs were washed and centrifuged after adding excess of ethanol. The obtained NPs were then dispersed in non-polar solvents.

The particle diameters and their distribution were measured by transmission electron microscopy (TEM) (300 keV, JEM 3010 microscope) at the Brazilian Synchrotron Light Laboratory (LNLS). The structure was determined by x-ray diffraction (XRD) (Philips, X-PERT) with Cu K α radiation and the magnetic properties were measured with a PPMS (Quantum Design) magnetometer installed with VSM option.

III. RESULTS AND DISCUSSION

Figures 1(a) and 1(b) shows the representative TEM images of the Ag–CoFe₂O₄ dimer NPs both in low as well as high resolution modes. One can see two different contrasts in the morphology of the majority of the particles. Here dark

^{a)}Electronic mail: surender76@gmail.com.

contrast corresponds to Ag NPs, whereas the light one corresponds to CoFe_2O_4 NPs [see Fig. 1(b)].⁷ The size distribution of the CoFe_2O_4 NPs in the Ag– CoFe_2O_4 NPs is around 13 (3) nm, whereas for Ag NPs, it is ~ 25 (7) nm. By the shape and morphology of the particles, we can infer that, in the second synthesis stage, CoFe_2O_4 grows using Ag NPs as pinning seeds, leading to the appearance of dimerlike particles [see Fig. 1(b)]. Figure 1(d) shows the representative XRD patterns of the Ag– CoFe_2O_4 NPs along with patterns for the Ag and CoFe_2O_4 reference NP samples. Here, one can clearly see that the pattern shows the strong contribution of the peaks indexed as Ag NPs encompassed by the very broad peaks indexed as CoFe_2O_4 spinel ferrite (cubic phase, $Fd3m$). It is observed that the peak positions shifted slightly to lower 2θ values for CoFe_2O_4 , which indicate the expansion of the lattice structure in case of dimer NPs. A detailed analysis of the peak positions and their relative intensities confirm a lattice expansion for the CoFe_2O_4 NPs that has been estimated to be 2.67(5) Å for the plane (311), which is approximately 3% and 5% larger than the corresponding values for the reference CoFe_2O_4 sample and standard bulk (2.53 Å, JCPDS No. 22-1086), respectively. On the other hand, there is no shifting in position of Ag peaks as compared to reference/standard bulk sample, which implies that lattice structure of Ag remains intact for the dimer NPs. Using the Scherrer formula, we have determined the effective crystalline size for the Ag [28 (1) nm] and CoFe_2O_4 [(5(1) nm) NPs. These values are in a close agreement with the values calculated from the TEM images of the Ag– CoFe_2O_4 NPs sample, in which a polycrystalline structure is observed.

Figure 2 shows the magnetization versus temperature curves for the reference CoFe_2O_4 and Ag– CoFe_2O_4 NPs

samples under zero-field-cooling (ZFC) and field-cooling (FC) modes. The low field (20 Oe) ZFC and FC magnetization curves for the CoFe_2O_4 NPs exhibit a blocking process typical of an assembly of weakly interacting randomly oriented NPs,⁸ where the M_{ZFC} show a narrow maximum at 35 K, which is associated with the mean blocking temperature $\langle T_B \rangle$ of an assembly of superparamagnetic (SPM) particles. The M_{FC} increases continuously as the temperature decreases, but below 20 K, it is practically constant up to the lowest measuring temperature. Conversely, in case of dimer NPs, the M_{ZFC} curve shows clearly two distinct contributions to the magnetization. At low temperatures (up to 30 K), the magnetization emerges due to the individual CoFe_2O_4 NPs (i.e., without the attached Ag NPs), and the M_{ZFC} shows a maximum at 26 K, which is slightly at lower temperature as compared to CoFe_2O_4 NPs reference sample. However, beyond it is added to the magnetic contribution of the dimer NPs leading to a very large energy barrier distribution, with blocking temperatures higher than 300 K. One can clearly see a clear separation between both ZFC and FC branches, which persist well above 300 K. At the same time, its M_{FC} part rises monotonically as the temperature decreases. The irreversibility temperature, T_{IRR} , is defined as the threshold temperature point above which ZFC and FC curves coincide. Therefore, when the values for both CoFe_2O_4 and Ag– CoFe_2O_4 NPs samples are compared, the T_{IRR} temperature rises from 145 K to above room temperature; which confirms the enhancement of the magnetic anisotropy.

Figure 3 shows the magnetization hysteresis loops for the Ag– CoFe_2O_4 and CoFe_2O_4 NPs sample at 2 K (maximum applied magnetic field up to ± 140 kOe). The reference CoFe_2O_4 NPs exhibit SPM behavior at room temperature,

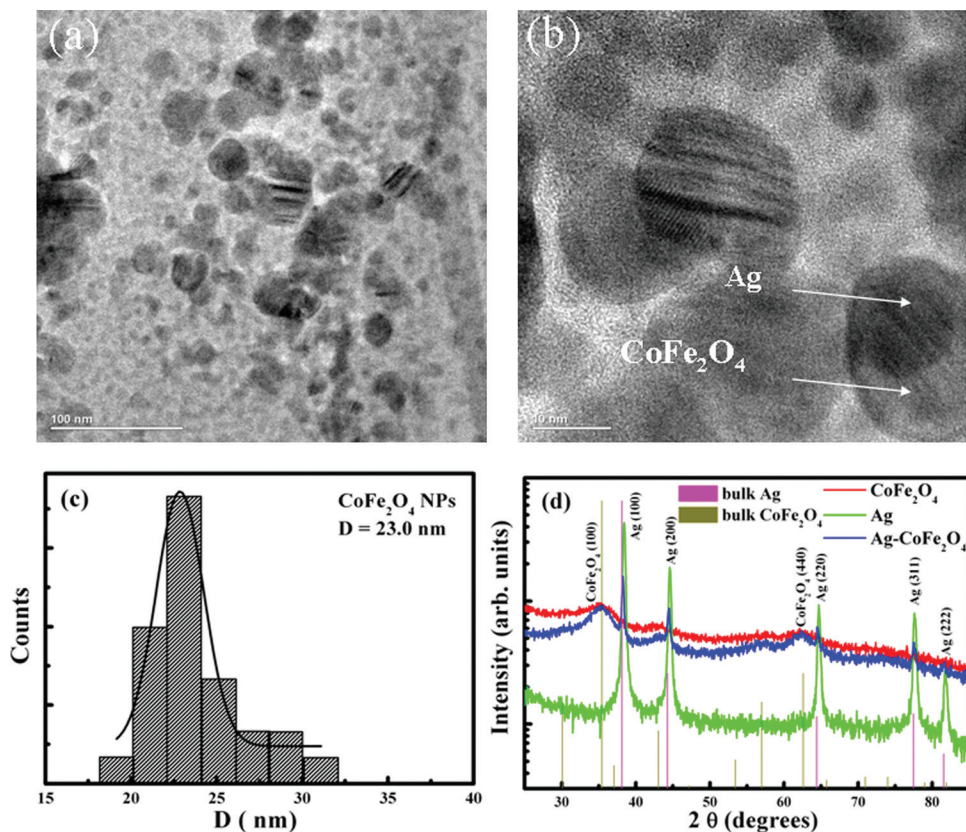


FIG. 1. (Color online) (a)–(b) TEM image of the Ag– CoFe_2O_4 NPs, (c) histogram of the particle size distribution for the reference CoFe_2O_4 NPs, and (d) powder XRD pattern for the references Ag and CoFe_2O_4 NPs, and Ag– CoFe_2O_4 NPs.

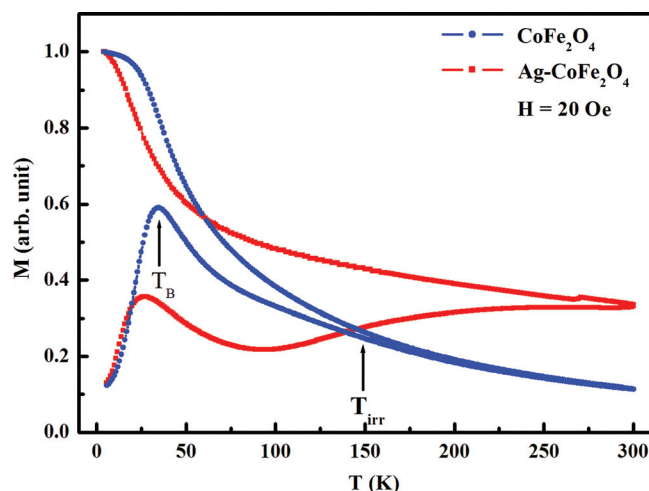


FIG. 2. (Color online) ZFC and FC magnetization for the CoFe_2O_4 and $\text{Ag-CoFe}_2\text{O}_4$ NPs sample.

whereas at 2 K the coercivity reaches a maximum value of 11.5 kOe, which is much larger than those of bulk cobalt ferrite (~ 5 kOe at 5 K). On the other side, the loop for the $\text{Ag-CoFe}_2\text{O}_4$ NPs sample shows two contributions: the high-field linear magnetic susceptibility and other ferromagnetic behavior at 2 K, which is similar to CoFe_2O_4 reference sample. However, the value of coercivity at 2 K increases from (11.5 kOe) for the CoFe_2O_4 NPs to 14.2 kOe for the dimer NPs. Additionally, compared with the magnetic field response of the CoFe_2O_4 reference sample, the enhancement of the magnetic anisotropy is evident through the observation of the nonsaturation magnetization of dimer NPs in a field of 140 kOe with a high-field linear magnetic susceptibility. Therefore, initially taking into account the structural morphology of the particles and the lattice expansion of the CoFe_2O_4 spinel phase in the dimer NPs, we believe that the mechanism behind the enhancement of the magnetic anisotropy and large coercivity result from the non-zero orbital moment, m_{orb} , and the related strong spin-orbit interaction.⁹ In addition, the distribution of cations between tetrahedral (A) and octahedral [B] sites in Co-ferrite, their chemical order, as well as deviation from the ideal (Co:Fe; 1:2) stoichiometry are known to affect considerably their magnetic properties. As the chemistry to fabricate reference and dimer NPs in the present case is slightly different, therefore the observed enhancement in the magnetic behavior of the dimer NPs could also be due to nonstoichiometric cobalt content or other structural-related defects.¹⁰ The investigations are under way to further tune, control, and optimize the magnetic response for the $\text{Ag-CoFe}_2\text{O}_4$ -type dimer NPs.

IV. CONCLUSION

We have synthesized $\text{Ag-CoFe}_2\text{O}_4$ dimer NPs by using a two-step chemical route. We have measured the magnetic

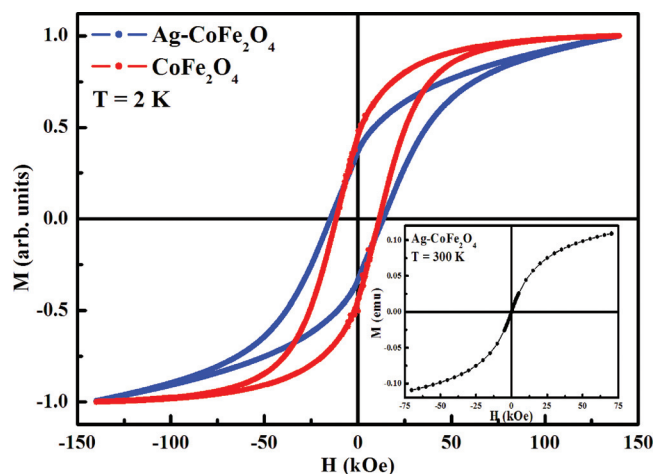


FIG. 3. (Color online) Hysteresis loops taken at 2 K for the CoFe_2O_4 and $\text{Ag-CoFe}_2\text{O}_4$ NPs sample in an applied field of ± 140 kOe. Inset shows the corresponding curve at 300 K for the $\text{AgCoFe}_2\text{O}_4$ NPs sample.

properties of reference CoFe_2O_4 NPs and $\text{Ag-CoFe}_2\text{O}_4$ dimer NPs. By means of dc magnetization measurements, we have been able to show the Ag due to its interface with CoFe_2O_4 ; the thermal stabilization of the dimer composite NPs enhanced and are greater than that of CoFe_2O_4 NPs alone. Taking into account the morphology of the dimer NPs and the lattice expansion of the CoFe_2O_4 phase, we believe that the mechanism behind the enhancement of the magnetic anisotropy and large coercivity at 2 K result could be ascribed to the interface effect between Ag and CoFe_2O_4 components and the related structural defects. This is closely connected with the lift of zero orbital moment, m_{orb} , and the related strong spin-orbit interaction.

ACKNOWLEDGMENTS

The authors are grateful to FAPESP and CNPq, Brazil for providing financial support. They would also like to thank LNLS for their support during TEM imaging.

- ¹Y. Sun and Y. Xia, *Science* **298**, 2176 (2002).
- ²C. Wang, Y. Wei, H. Jiang, and S. Sun, *Nano Lett.* **9**, 4544 (2009).
- ³G. Lopes, J. M. Vargas, S. K. Sharma, F. Beron, K. R. Pirota, M. Knobel, C. Rettori, and R. D. Zysler, *J. Phys. Chem. C* **114**, 10148 (2010).
- ⁴H. Hori, Y. Yamamoto, T. Ywamoto, T. Miura, T. Teranishi, and M. Miyake, *Phys. Rev. B* **69**, 174411 (2004).
- ⁵A. Jordan, R. Scholz, P. Wust, H. Fahling, and R. Felix, *J. Magn. Magn. Mater.* **201**, 413 (1999).
- ⁶G. F. Goya, V. Grazu, and M. R. Ibarra, *Curr. Nanosci.* **4**, 1 (2008).
- ⁷H. Yu, M. Chen, P. M. Rice, S. X. Wang, R. L. White, and S. Sun, *Nano Lett.* **5**, 379 (2005).
- ⁸D. Peddis, C. Cannas, G. Piccaluga, E. Agostinelli, and D. Fiorani, *Nanotechnology* **21**, 125705 (2010).
- ⁹M. C. Desjonquères, C. Barreateau, G. Autés, and D. Spanjaard, *Phys. Rev. B* **76**, 024412 (2007).
- ¹⁰G. Salzar-Alvarez, R. T. Olsson, J. Sort, W. A. A. Macedo, J. D. Ardisson, M. D. Baró, U. W. Gedde, and J. Nogués, *Chem. Mater.* **19**, 4957 (2007).